Journal of Anatomy

J. Anat. (2017) doi: 10.1111/joa.12666

Comparative cranial ontogeny of *Tapirus* (Mammalia: Perissodactyla: Tapiridae)

S. Rocio Moyano[1,2] and Norberto P. Giannini[3,4]

[1]*Consejo Nacional de Investigaciones Científicas y Técnicas (CONICET), San Salvador de Jujuy, Jujuy, Argentina*
[2]*Centro de Estudios Territoriales Ambientales y Sociales, Facultad de Ciencias Agrarias, Universidad Nacional de Jujuy, San Salvador de Jujuy, Jujuy, Argentina*
[3]*Unidad Ejecutora Lillo. Consejo Nacional de Investigaciones Científicas y Técnicas, San Miguel de Tucumán, Argentina*
[4]*Department of Mammalogy, American Museum of Natural History, New York, USA*

Abstract

Skull morphology in tapirs is particularly interesting due to the presence of a proboscis with important trophic, sensory and behavioral functions. Several studies have dealt with tapir skull osteology but chiefly in a comparative framework between fossil and recent species of tapirs. Only one study examined an aspect of cranial ontogeny, development of the sagittal crest (Holbrook. *J Zool Soc Lond* 2002; 256; 215). Our goal is to describe in detail the morphological changes that occur during the postnatal ontogeny of the skull in two representative tapir species, *Tapirus terrestris* and *Tapirus indicus*, and to explore possible functional consequences of their developmental trajectories. We compared qualitative features of the skull on a growth series of 46 specimens of *T. terrestris* ordered on the basis of the sequence of eruption and tooth wear, dividing the sample into three age classes: class Y (very young juvenile), class J (from young juvenile to young adult) and class A (full and old adult). The qualitative morphological analysis consisted of describing changes in the series in each skull bone and major skull structure, including the type and degree of transformation (e.g. appearance, fusion) of cranial features (e.g. processes, foramina) and articulations (sutures, synchondroses, and synovial joints). We then measured 23 cranial variables in 46 specimens of *T. terrestris* that included the entire ontogenetic series from newborn to old adults. We applied statistical multivariate techniques to describe allometric growth, and compared the results with the allometric trends calculated for a sample of 25 specimens of *T. indicus.* Results show that the skull structure was largely conserved throughout the postnatal ontogeny in *T. terrestris*, so class Y was remarkably similar to class A in overall shape, with the most significant changes localized in the masticatory apparatus, specifically the maxillary tuber as a support of the large-sized permanent postcanine dentition, and correlated changes in diastemata, mandibular body, and sagittal and nuchal crests. In the nasal region, ontogenetic remodeling affected the space for the meatal diverticulum and the surfaces for the origin of the proboscis musculature. Overall, ontogenetic trajectories exhibited more negative allometric components in *T. indicus* than in *T. terrestris*, and they shared 47.83% of allometric trends. *Tapirus indicus* differed most significantly from *T. terrestris* in the allometry of postcanine toothrows, diastemata and mandibular body. Thus, some allometric trends seem to be highly conserved among the species studied, and the changes observed showed a strong functional and likely adaptive basis in this lineage of ungulates.

Key words: morphology; ontogeny; perissodactyla; proboscis; skull; tapir; *Tapirus indicus*; *Tapirus terrestris*.

Introduction

The South American tapir *Tapirus terrestris* (Linnaeus, 1758) is an ungulate mammal that belongs in the Perissodactyla. Tapiridae is the only extant family in the mostly extinct Tapiroidea, with the single genus *Tapirus* and four currently recognized extant species: *Tapirus terrestris, Tapirus pinchaque, Tapirus bairdii* and *Tapirus indicus* (Wilson & Reeder, 2005). A fifth, newly described species of South American tapir (*Tapirus kabomani,* Cozzuol et al. 2013) has been seriously questioned on the basis of molecular data, and the involved specimens may in fact belong in *T. terrestris* (Voss et al. 2014). Three species are distributed in the Neotropics and one, the Malayan tapir *T. indicus*, in Southeastern Asia (Wilson & Reeder, 2005). Phylogenetic analyses suggest that extant New World tapirs are more closely

Correspondence
S. Rocio Moyano, Facultad de Ciencias Agrarias, UNJu, Centro de Estudios Territoriales Ambientales y Sociales (CETAS). Alberdi 47, Y4600DTA San Salvador de Jujuy, Jujuy, Argentina.
E: s.rociomoyano@gmail.com

Accepted for publication *2 June 2017*

related to each other than either is to the Malayan tapir, and that *T. pinchaque* is sister to *T. terrestris* (Norman & Ashley, 2000). The latter two species possess a ridge along the sagittal midline of the skull, whereas the other two living species of the genus present a pair of temporal parasagittal lines forming the lateral boundaries of a planar sagittal table. The crest in *T. pinchaque* is small and divided to form a triangular table on the occiput (Padilla & Dowler, 1994); in *T. terrestris* the crest is notably high and narrow resembling a helmet in lateral view (Holbrook, 2002). *Tapirus bairdii* and *T. indicus* lack a median sagittal crest and present paired parasagittal ridges on the dorsolateral aspect of the braincase instead, which form the lateral boundaries of the parasagittal table (Holbrook, 2002).

As large phytophagous mammals, extant tapirs retained plesiomorphic browsing habits, which requires extensive mastication of large quantities of foliage of relatively low protein content (Janis, 1995) and/or heavily chemically defended. These demands are reflected in the skull and dentition: browsers and particularly tapirs exhibit large brachyodont molars, large temporal fossae, and a well-developed nuchal (= lambdoid) crest (Holbrook, 2002). However, the most prominent feature of their head morphology is the presence of a short, mobile proboscis. A proboscis is narrowly defined as a flexible narial and upper lip extension with food grasping function (Milewski & Dierenfeld, 2013). Interestingly, by that definition tapirs are the only extant mammals, besides elephants, that possess a true proboscis (Milewski & Dierenfeld, 2013). The proboscis is considered a case of evolutionarily novel narial anatomy, a highly modified organ that is best interpreted as a muscular hydrostat (Witmer et al. 1999). In addition, this organ has tactile function, with sensory vibrissae (Padilla & Dowler, 1994; Kemp, 2005), and it has a role in social interactions (see Gwynne & Bell, 1968; Bell, 1969, 1970; Jarman, 1974; Owen-Smith, 1982; Janis & Ehrhardt, 1988). The proboscis is composed almost entirely of soft tissues and there is an evolutionary replacement of the rigid mammalian structure of nasal bone and cartilage by an organ constructed of connective tissue and specialized muscles (Witmer et al. 1999). The only cartilaginous support is a septal cartilage forming the roof and rostral portion of the proboscis, which extends caudally and then laterally to form a meatal diverticulum of no obvious function and uncertain homology (Witmer et al. 1999).

In evolutionary terms, the presence of a proboscis has been related with changes in three fundamental skull features (Radinsky, 1965, 1966, 1969): (1) expansion of the nasal incision, forming the meatal diverticulum [considered by Wall (1980) as a prerequisite for the origination of a mobile proboscis); (2) loss of the nasal process of the premaxilla and its contact with the nasal (i.e. the nasoincisive suture missing); and (3) shortening of the nasal bone. These features are present in tapirs and are among the features that together distinguish tapirs as a group from other perissodactyls, as well as from most other extant ungulates.

There are many morphological studies on the group, including ones on cranial osteology, although the latter were conducted chiefly within a comparative framework of extant vs. fossil forms (e.g. Hatcher, 1896; Simpson, 1945; Hershkovitz, 1954; Holanda, 2007). Two studies considered aspects of nasal morphology, describing the arrangement of turbinal bones (Paulli, 1900) and, more recently, the anatomical structure of the proboscis (Witmer et al. 1999). Some describe the general anatomy (e.g. Parker, 1882; Beddard, 1909), whereas other studies have dealt with age classes on the basis of craniodental characters as applied to conservation of the focal species (e.g. Maffei, 2003). Only one paper describes an aspect of cranial ontogeny in tapirs, but it is restricted to the development of the sagittal crest as a significant systematic character (Holbrook, 2002). A comprehensive ontogenetic study of the tapir skull is lacking. However, this topic is of potentially great interest for understanding the evolution of specializations such as the proboscis in mammals. How these and other characters develop in extant tapirs is the key to advancing the comparative study of these and other taxa known or inferred to have a short proboscis (Radinsky, 1965; Wall, 1980).

In this study we describe in detail the cranial morphology of a growth series of the South American tapir *T. terrestris*, and determine, on a qualitative basis, the ontogenetic changes that take place during the postnatal developmental period, when the crucial dietary change from lactation to a herbivorous browsing diet occurs. We explore the most significant morphofunctional consequences of our results, and quantitatively estimate growth of skull components from a large ontogenetic series of *T. terrestris* using a multivariate allometry approach, establishing a comparative basis with data from the closely related Malayan tapir *T. indicus*.

Materials and methods

The species

This study is based on our main sample of 46 specimens of the common tapir *Tapirus terrestris*, also known as anta, danta, lowland tapir or Brazilian tapir, which is the species of Tapiridae with the widest distribution, ranging from northern South America to Northern Argentina. No specimens assigned to *T. kabomani* are included in this sample (see specimen list below). *Tapirus terrestris* is a large (150–250 kg; Padilla & Dowler, 1994) mammalian herbivore with high conservation value. The International Union for Conservation of Nature (IUCN) qualifies *T. terrestris* as vulnerable to extinction globally, with few regional strongholds where the species survives in good condition (Naveda et al. 2008). This species is considered a 'landscape architect' due to its intense activity along trails, which transforms the physiognomy of vegetation (Taber et al. 2008). An additional ecological function relates to its influence on forest dynamics because of its impact on seed dispersal and seedling and treelet predation. Numerous studies have been made in a conservation context (e.g. Bodmer, 1990; Bodmer & Brooks, 1997; Ayala, 2003; de Bustos et al. 2004; among others).

We compared the results obtained from *T. terrestris* (see below) with those from a sample of 25 specimens of *T. indicus*, which is the only Old World species in the genus and is a contrasting species in several respects (see Holbrook, 2002). The Malayan tapir is native to the Malay Peninsula and Sumatra, and it may have been present until recently in Borneo; it is categorized as endangered (Traeholt et al. 2016). *Tapirus indicus* is the largest species and the one with the longest proboscis (Witmer et al., 1999). Likely, most ecological and behavioral traits are comparable to those of the Neotropical tapirs.

Qualitative analysis

We examined a series of 71 skulls of *T. terrestris*. These specimens are housed in the American Museum of Natural History (AMNH; New York, USA), the National Museum of Natural History, Smithsonian Natural Institution (USNM; Washington, DC, USA), Field Museum of Natural History (FMNH; Chicago, USA), Colección Mamíferos Lillo (CML; Tucumán, Argentina), Museo Argentino de Ciencias Naturales 'Bernardino Rivadavia' (MACN; Buenos Aires, Argentina) and Museo Nacional de Historia Natural (MNHN; Montevideo, Uruguay).

The specimens were arranged to form an ontogenetic series following the sequence of eruption and tooth wear observed in the sample (Fig. 1). For the analysis of the changes that occurred during cranial growth and types and transformation degrees (e.g. fusion) of cranial joints, we divided the specimens of the sample following a dental eruption key of Gibson (2011). We examined the upper dentition and, for qualitative comparative purposes only (see below for quantitative, continuous-scale analyses of skull ontogeny), we preferred to divide the specimens into three age classes, from incomplete dentition to complete dentition:

Class Y (very young juvenile): from unerupted tooth to DP4 not yet fully erupted. No sign of molars

Class J (from young juvenile to young adult): DP1–DP4 are all fully erupted and permanent premolars and molars begin to emerge. The third molar is patent but has not fully emerged

Class A (full and old adult): all dental elements fully erupted.

These classes comprise individuals of various ages: specimens of Class Y included individuals under 1 year of age, Class J included individuals between 1 and 6 years; and Class A included individuals older than 6 years (see Gibson, 2011).

We analyzed different constituent parts of the skull regions and bones to reconstruct the changes that occur during the postnatal ontogeny. We examined each rostral (premaxilla, maxilla, nasal, jugal or zygomatic, lacrimal, palatine, pterygoid, vomer) and cranial (frontal, parietal, sphenoid complex, squamosal, petrosal, ectotympanic, tympanohyoid, occipital complex, mandible) bones with the exception of turbinates and auditory ossicles (poorly preserved in our sample). These bones are illustrated in intact skulls in Figs 2–10. We summarized changes in overall appearance, shape, surface texture, and other remarkable features, per bone and skull region. We also report changes in cranial joints, foramina, and key structures such as processes, ridges, and other features along the ontogenetic series (Fig. 11). Anatomical terminology followed Evans (1993). Abbreviations used throughout the text are listed in Table 1.

The following specimens of *T. terrestris* are used in this study [specimens used in quantitative analysis only, are in italics (see below); specimens used in qualitative analysis only, are in parentheses, all other specimens are included in both analyses]:

Class Y: AMNH 202838; CML 4933, 8139; *23547*, *100133*; FMNH: *60441*; MACN: 4.339, 52.77; (MACN 4.386, 11.11, 25.34, 25.35, 26.70, 36.139, 52.77, 48.329, 48.330); USNM: 143861

Class J: CML: 8137, *9828, 9820, 9821, 9823*; (CML 6347, 8138); FMNH: *87882, 21377, 88794, 95385, 140281, 87883*; MACN: 28.89, 7.6, 10.24, 10.25*, 25837, 29.854, 31.211, 47.380, 49.322, 47.386, 23530*; (MACN: 9.46, 47.386, 25.44, 4.273, 33.221, 29.854, 47.380, 49.322, 23530); MNHN: 701, 702, 800, 2230

Class A: CML: 24.30, 9817, 9818, 9819, *9829, 9830*; (CML 06346, 9829); FMNH: *60768, 134499*; MACN: 4.329, 10.26, 25836, 33.276, 50.559; MNHN: 703.

Quantitative (allometric) analysis

For this analysis, the growth series is taken as a continuum. We analyzed a large postnatal ontogenetic series of 46 specimens of *T. terrestris*. Our sample covers all stages in the ontogenetic series of *T. terrestris.* The sample comprised seven very young juvenile specimens, of which the smallest one was 163.99 mm in condyle-basal length (AMNH 202838), 27 young juvenile to adults, and 12 full and old adults, of which the largest specimen was 399.76 in condyle-basal length (MACN 33.276).

Allometry, in morphometric studies, refers to the association between size and shape variation (Huxley, 1932; Mosimann, 1970; Gould, 1977; Mitteroecker et al. 2013). Allometry of size compares shape changes with overall size along a growth series (i.e. rate of development vs. rate of growth) in which the time frame is implicit (see Abdala et al. 2001). In particular, ontogenetic allometry (or growth allometry) deals with covariation among characters as the organism grows (Klingenberg & Zimmermann, 1992; Klingenberg, 1996).

We used 23 linear measurements (Fig. 12) to describe skull components in all specimens of the ontogenetic series. The craniomandibular dimensions analyzed here, partially overlap with those considered in other morphometric studies of mammalian skulls (Abdala et al. 2001; Giannini et al. 2004, 2010; Cassini et al. 2012, 2015; Flores et al. 2013; Tarnawski et al. 2014a,b, 2015). To estimate growth trends, we used multivariate analyses based on the generalized allometry equation originally proposed by Jolicoeur (1963). Here, size is regarded as a latent variable affecting all measurements simultaneously (Flores et al. 2006), and the first eigenvector of a principal component analysis (PCA) expresses the various allometric relationships of the chosen variables. This vector is extracted from a variance-covariance matrix of log-transformed variables and scaled to unity. For a given variable, allometry is a deviation of its corresponding eigenvector element with respect to a hypothetical isometric value that represents isometry of all variables (i.e. pure size change). The expected isometric value is calculated as the square root of $1/p$ with p equal to the number of variables. In our study the hypothetical isometric value is 0.208 for 23 skull variables.

To estimate the statistical departures from isometry, we used the application of the jackknife (Quenouille, 1956; Manly, 1997) developed by Giannini et al. (2004), which generates confidence intervals (CI) for each of the empirically derived first-eigenvector elements (Giannini et al. 2010). The CI may be inclusive of the null value (here 0.208) and therefore the variable is considered statistically indistinguishable from isometry. Alternatively, the CI may exclude this value and therefore be considered significantly allometric: 'positive' if the observed element is > 0.208, or 'negative' otherwise. To calculate this confidence interval, n pseudo samples are generated such that a new first unit eigenvector is calculated from a matrix with one specimen removed at a time (with n equal to the number of

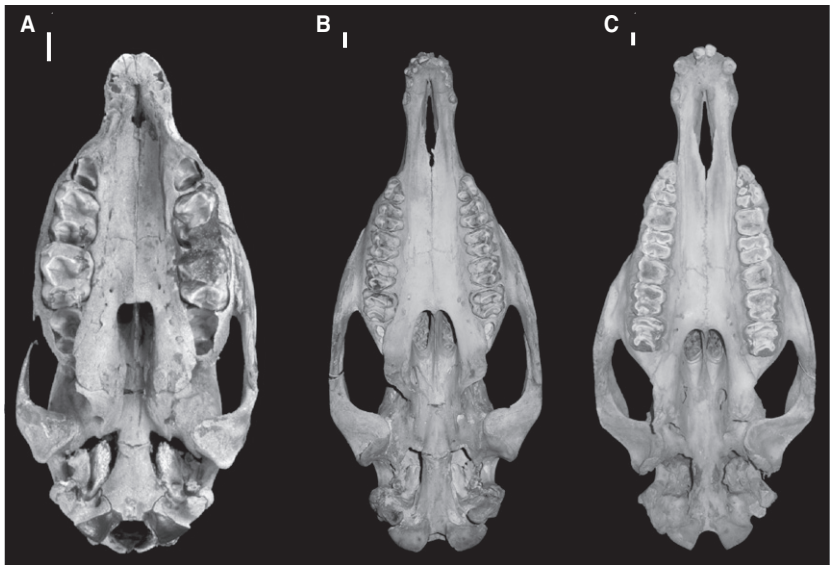

Fig. 1 Skull of *Tapirus terrestris* in ventral view representing the three age classes: (A) Class Y (AMNH 202838); (B) class J (MACN 52.77); and (C) class A (MACN 33.276). Scale bar: 10 mm.

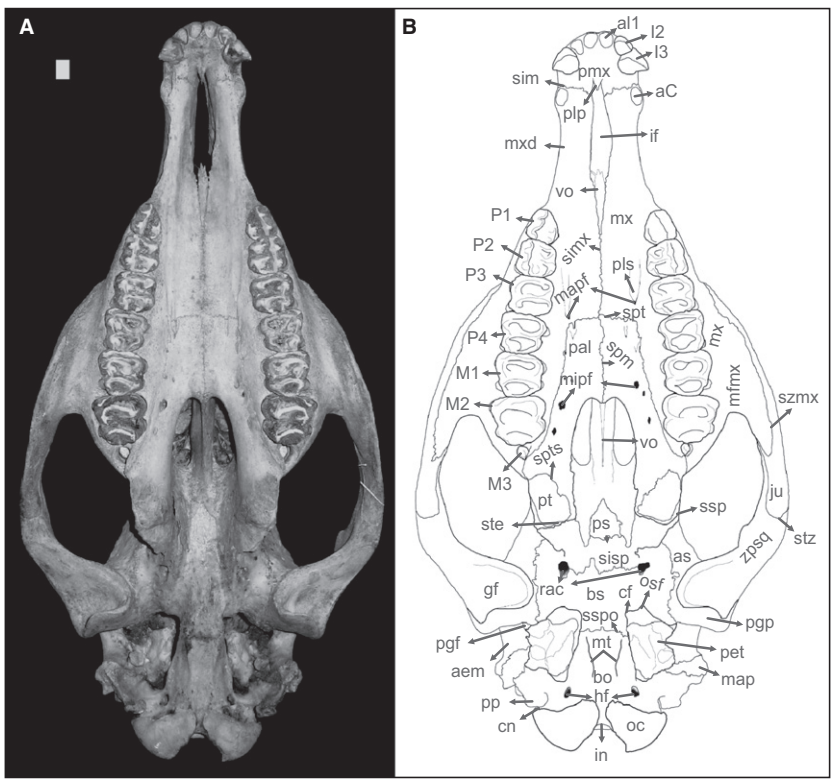

Fig. 2 (A) Skull of *Tapirus terrestris* (MACN 31.211) in ventral view. (B) Line drawing of (A). Abbreviations as in Table 1. Scale bar: 10 mm.

specimens). Here we report untrimmed (full set of jackknife pseudovalues used) and trimmed calculations (with the *m* smallest pseudovalues removed in the calculations, with $m = 1$), the latter being used to test whether extreme pseudovalues affected the CI estimation (Manly, 1997). We report the 95% CI for each allometry coefficient (for more details see Giannini et al. 2004). The multivariate statistical analysis (PCA + jackknife resampling; Giannini et al. 2010) was programmed in an R script (R Development Core Team 2015) and is available from the authors.

We integrated the results obtained from the developmental series of *T. terrestris* with an identical analysis of a postnatal ontogenetic series of 25 specimens of *T. indicus*. The *T. indicus* sample comprised five very young juvenile specimens, of which the smallest specimen was 276.29 mm in condyle-basal length (USNM 267365), 11 young juveniles to young adults, and nine full adults and old adults, of which the largest specimen was 458.82 mm in condyle-basal length (FMNH 60010). The following specimens of *T. indicus* are used in this study:

Class Y: AMNH: 137309, 167844; FMNH: 41393; MACN: 12.9; USNM: 267365

Class J: AMNH: 14106, 35661; FMNH: 66016, 66017, 93698; MACN: 12.9, 25.53, 30.351, 28.89; USNM: 267510, 308734, 14648

Class A: AMNH: 130108, 201799, 54960, 180030; FMNH: 60010, 123664; MACN: 29.926; USNM: 283565, 155410.

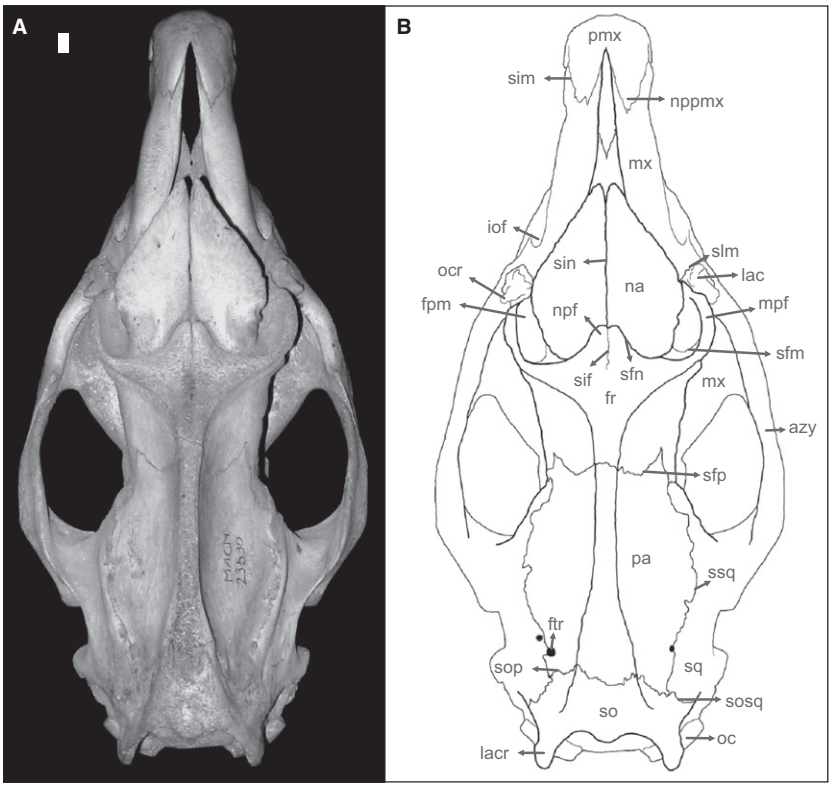

Fig. 3 (A) Skull of *Tapirus terrestris* (MACN 23530) in dorsal view. (B) Line drawing of (A). Abbreviations as in Table 1. Scale bar: 10 mm.

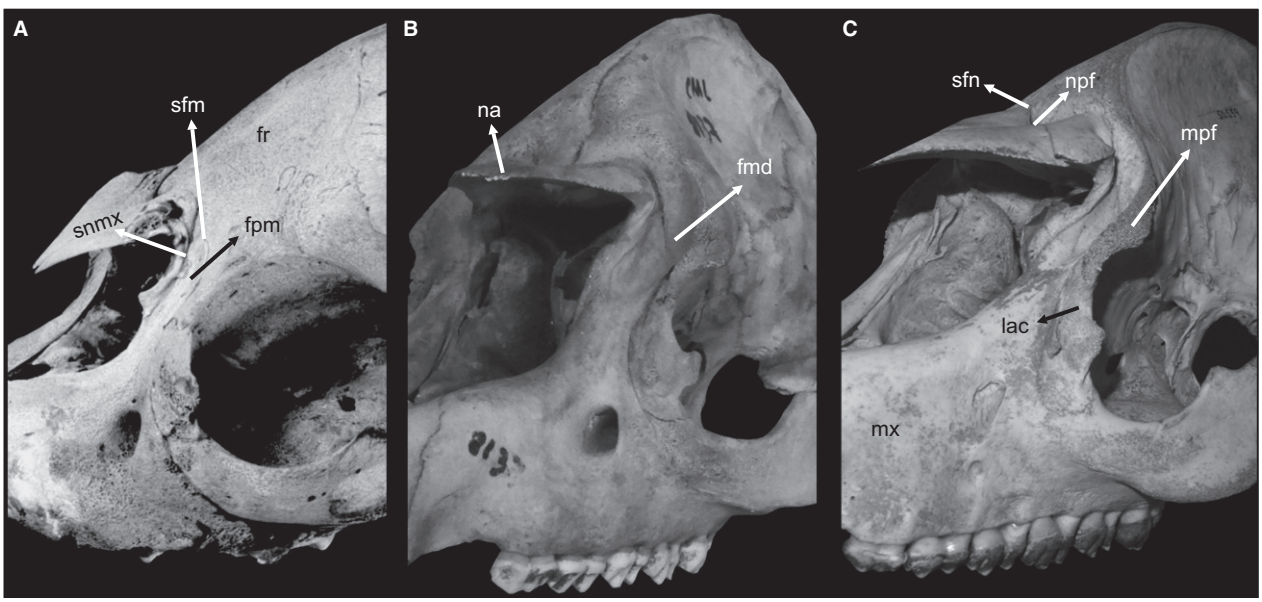

Fig. 4 Skull of *Tapirus terrestris* in oblique view to show the nasal region. (A) Class Y (AMNH 202838). (B) Class J (MACN 29.854); and (C) Class A (MACN 50.559). Abbreviations as in Table 1.

Results and Discussion

Qualitative analysis: the skull bones

Rostral bones

The main changes during the ontogeny of the rostral bones are summarized in Table 2. The majority of these changes contributed to the elongation of the muzzle and the maxillary diastema (Figs 1, 4 and 10), which produced a relative tapering of the muzzle (a probable advantage for browsing mammals; see Owen-Smith, 1982); development of maxillary tuber (see below and Figs 1 and 2); and development of the proboscis area (Figs 3 and 4), which are associated with reported browsing habits in the species, as well as with

social interactions (see Gwynne & Bell, 1968; Bell, 1969, 1970; Jarman, 1974; Owen-Smith, 1982; Janis & Ehrhardt, 1988).

The nasal region is retracted in the tapir, and highly variable in shape across specimens. In general, the left and right nasals fuse toward adulthood to compose a single, heart-shaped bone that is relatively wide with respect to the nasals in class Y. As compared with other ungulates, the nasals are reduced in the tapir and so the bulk of the rostrum is represented by the premaxilla and maxilla (Figs 1, 5, and 10). The posterior part of the latter, in the floor of the orbital region, is occupied by the large maxillary tuber, one of the skull regions that exhibit the greatest ontogenetic changes (Figs 1 and 2). The posteriorly exposed tuber houses most of the cheek dentition in the tapir, the deciduous and permanent premolars, and principally the permanent molars. These elements are added ontogenetically one by one in a rostrocaudal sequence (from P4 to M3). When the deciduous premolars are replaced by permanent premolars (which are of comparable size, shape and inferred function to the deciduous set), and the molars emerge, considerable growth is patent toward the caudal end of the maxillary tuber. This involved a massive remodeling of the maxilla, due especially to the relative large volume of the permanent molars, and remarkably very little ontogenetic change in the palatal surface. This was evident also in the relative position of some dental elements, particularly P4, which is displaced anteriorly, and the end of the toothrow, which widens considerably to hold the successively emerging molars. In class Y, the pterygoid bone presented a small and rounded tuber from which the veli tensor muscle of the palate originates (Sisson & Grossman, 1982). The pterygoid developed into a hook-shaped hamulus in some (e.g. MACN 9.46) but not all (e.g. CML 9830) specimens of class A.

The origin of the important caninus muscle originates in a slightly porous surface located caudoventral to the infraorbital foramen in the maxillozygomatic suture; this muscle depresses the elevated proboscis and contributes to lateral flexion and twisting of the proboscis during unilateral contraction (Witmer et al. 1999). This area was indistinct in class Y (e.g. AMNH 202838) but became evident in older specimens.

The lacrimal bone exhibited a relatively featureless surface in the smallest (class Y) specimens (e.g. AMNH 202838; Figs 5 and 10), with two large lacrimal foramina opening posteriorly in the orbital edge of the bone. The lacrimal is considerably roughened in class A, presenting a medial sulcus along the maxillolacrimal suture associated with the levator labii superioris muscle, the largest levator of the proboscis when acting bilaterally (chiefly originating in the large anterolateral tuberosity of the frontal), and two prominent tuberosities for the origin of the malaris, levator

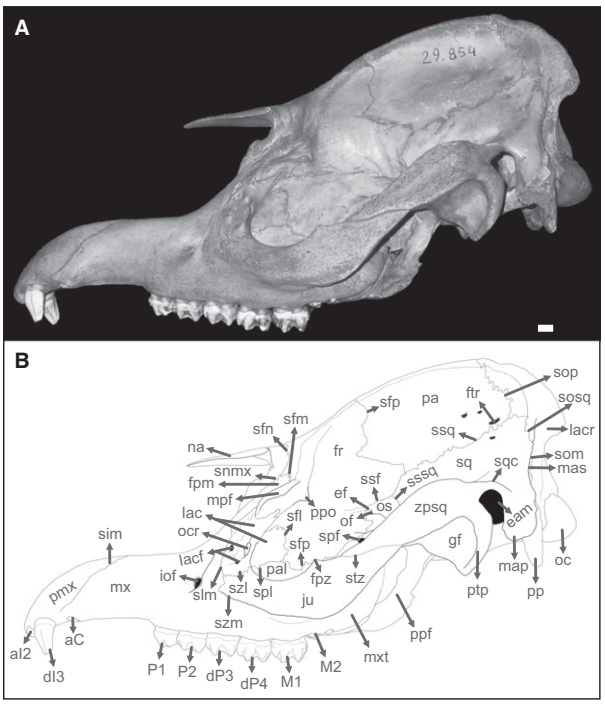

Fig. 5 (A) Skull of *Tapirus terrestris* (MACN 29.854) in left lateral view. (B) Line drawing of (a). Abbreviations as in Table 1. Scale bar: 10 mm.

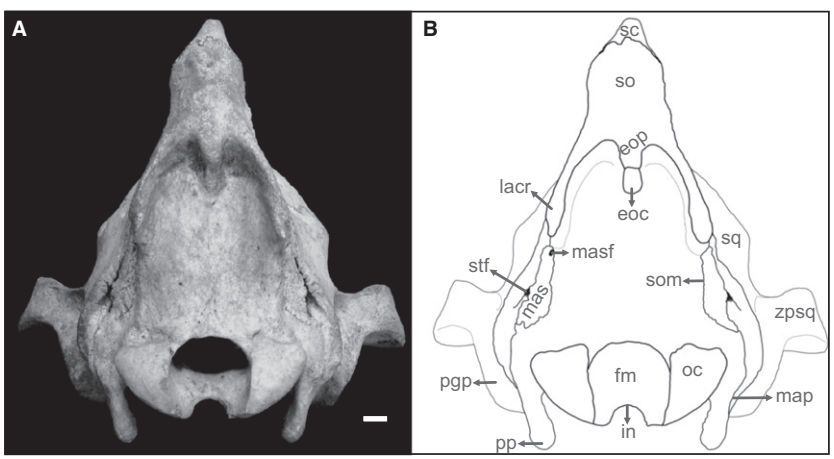

Fig. 6 (A) Skull of *Tapirus terrestris* (CML 06347) in occipital view. (B) Line drawing of (A). Abbreviations as in Table 1. Scale bar: 10 mm.

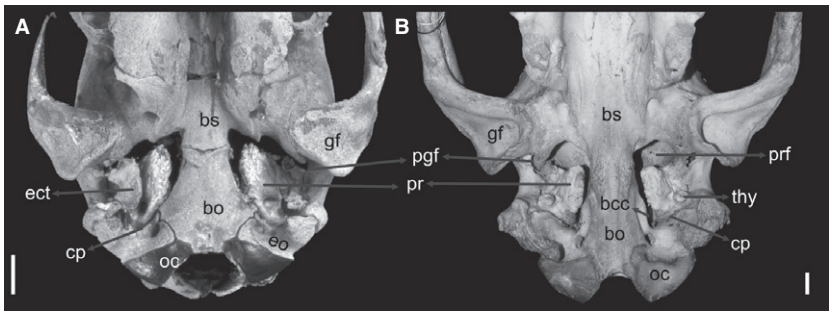

Fig. 7 Skull of *Tapirus terrestris* in ventral view, showing the petrosal, ectotympanic and tympanohyoid. (A) Class Y (AMNH 202838); (B) Class A (MACN 50.559). Abbreviations as in Table 1. Scale bar: 10 mm.

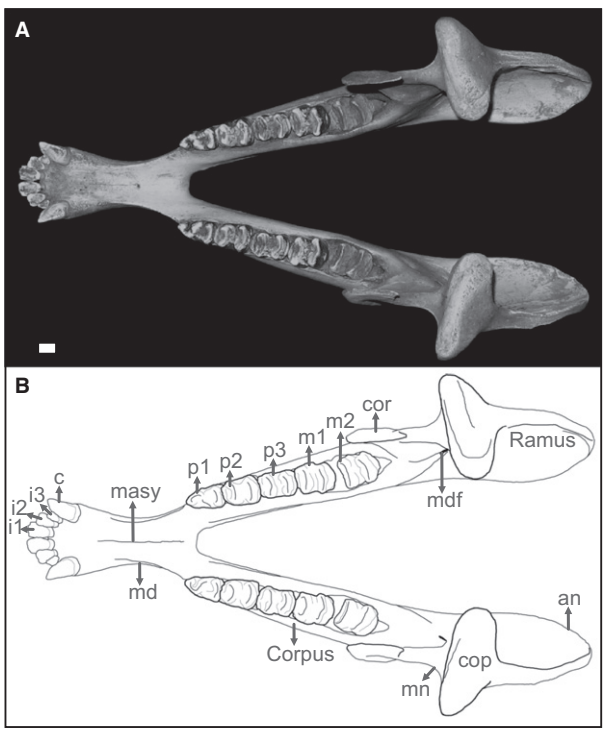

Fig. 8 (A) Mandible of *Tapirus terrestris* (MACN 47.380) in dorsal view. (B) Line drawing of (a). Abbreviations as in Table 1. Scale bar: 10 mm.

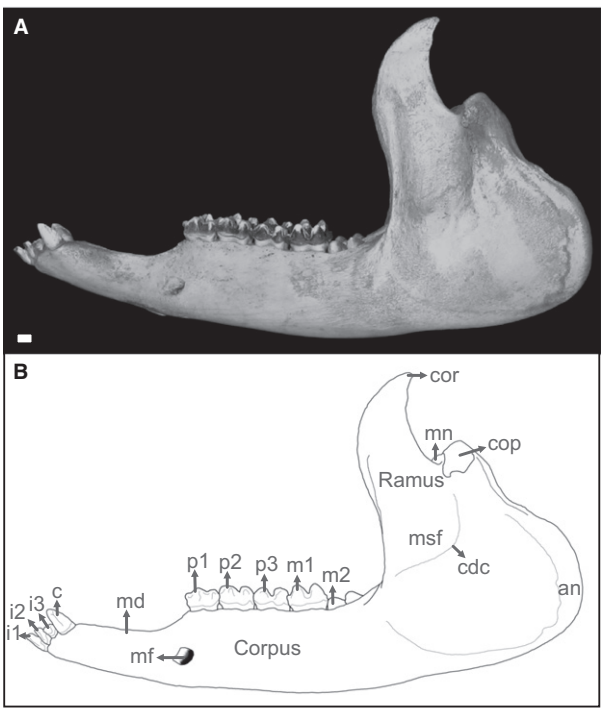

Fig. 9 (A) Mandible of *Tapirus terrestris* (MACN 47.380) in left lateral view. (B) Line drawing of (A). Abbreviations as in Table 1. Scale bar: 10 mm.

anguli oculi medialis and levator nasolabialis muscles (Witmer et al. 1999).

The fossa for the meatal diverticulum is a remarkable feature of the tapir skull (Fig. 4). The meatal diverticulum is a mucocartilaginous pouch controversially homologized with the nasal diverticulum of the horse (see Witmer et al. 1999). The frontal, maxillary, and nasal surfaces that form the fossa for the diverticulum deepen considerably, throughout development, from a shallow fossa not reaching the nasals in class Y, to a lyre-shaped, deep fossa in class A, surrounded by sharp lateral ridges. The meatal diverticulum of full and old adults overlaps the nasal surface as a lobe and leaves a rounded impression on its surface (Fig. 4). In class J, the frontal participates in forming a robust lateral wall (Fig. 4). This robust lateral margin of the fossa serves as origin for the levator anguli oculi medialis, orbicularis oculi, and orbitalis fascia muscles (Witmer et al. 1999).

Cranial bones

Braincase. The main changes that could be reconstructed along the ontogeny of the cranial bones are summarized in the Table 3.

These changes were associated with the origin of muscles in the sagittal and nuchal (= lambdoid) crests. We observed in the earliest specimen (AMNH 202838; without any erupted deciduous premolars) a globular braincase with no signs of sagittal crest. In class Y with third dP3 erupted (MACN 25.35) we observed that the crest simply erupts from the midline skull. The sagittal crest continues to heighten throughout development. In class A, a

Fig. 10 Skull of *Tapirus terrestris* in left lateral view. (A) Class Y (AMNH 202838); (B) class J (MACN 47.380); and (C) class A (MACN 33.276). Scale bar: 10 mm.

	Joints	Figure	Y	J	A
	Sutures				
Rostral	1.Incisivomaxillaris	1, 2, 3, 5, 10			
Rostral	2.Palatolacrimalis	5, 10			
Rostral	3.Nasomaxillaris	5, 10			
Rostral	4.Internasalis	3			
Rostral	5.Lacrimomaxillaris	5, 10			
Rostral	6.Zygomaticomaxillaris	5, 10			
Rostral	7.Zygomaticolacrimalis	5, 10			
Rostral	8.Intermaxillaris	1, 2			
Rostral	9.Patina transversa (=palatomaxillaris)	1, 2			
Rostral	10.Palatina mediana (=interpalatina)	1, 2			
Rostral	11.Interincisive (= interpremaxillaris)	1, 2			
Rostral	12.Pterygosphenoidalis	1, 2			
Rostral	13.Pterygopalatina	1, 2			
Cranial	14.Sphenofrontalis	5, 10			
Cranial	15.Sphenosquamosa	5, 10			
Cranial	16.Frontonasalis	3, 5, 10			
Cranial	17.Frontomaxillar	5, 10			
Cranial	18.Frontolacrimalis	5, 10			
Cranial	19.Temporozygomatica	5, 10			
Cranial	20.Occipitosquamosa	5, 10			
Cranial	21.Squamosa	5, 10			
Cranial	22.Frontoparietalis	3, 5, 10			
Cranial	23.Occipitoparietalis	3, 5, 10			
Cranial	24.Frontopalatina	5, 10			
Cranial	25.Sphenopalatina	5, 10			
Cranial	26.Occipitomastoidea	5, 6, 10			
Cranial	27.Sagittalis (=interparietalis)	3			
Cranial	28.Interfrontalis	3			
	Synchondroses				
	1. Spheno-occipitalis	1, 2			
	2. Intersphenoidalis	1, 2			
	3. Symphysis of the mandible	8			
	4. Intraoccipitalis	1, 2			

Foliate suture · Squamous suture · Plane suture
Serrated suture · Partially fused · Fused

Fig. 11 Changes in skull and mandible joints between the three age classes (Y, J, and A classes) of specimens of *Tapirus terrestris*, indicating the figure where character is observed.

prominent sagittal crest has developed in the skull midline comprising the frontal, parietal, and supraoccipital (interparietal not observed in specimens of our sample; Figs 3 and 10). In no other tapir species does the sagittal crest achieve such a degree of development, around which a particularly strong temporalis muscle originates (Holbrook, 2002). The final shape of the sagittal crest, in dorsal view, is that of a thick table that gently expanded both anteriorly into the nasal area, and posteriorly to join the nuchal crest. The latter also developed strongly with two main features. First, the growth of the nuchal crest appeared restricted to the dorsal half of the supraoccipital so that it projected posteriorly from the dorsal part of the occiput only (Fig. 6); these bilateral lines were slight but well-marked in class Y (not shown). Secondly, a marked midline protuberance, as seen in posterior view, became a strong external occipital protuberance, and continued ventrally in a short and low external occipital crest (Fig. 6). Radinsky (1965) associated the enlarged occipital crests with neck musculature and the nuchal ligament that support large skulls in species bearing a proboscis. In the smallest specimens, a very young juvenile AMNH 202838 and MACN 4.339, the left and the right exo-occipitals fail to contact each other in the midline, and even a small indentation is present in the supraoccipital in this point (Fig. 6); this condition is rapidly lost in larger specimens, in which the three bones fuse seamlessly.

Skull base. The most notable ontogenetic change in the skull base was the elongation of the basioccipital (Figs 1 and 2). In class Y, this bone is trapezoidal in shape in ventral view, with a slightly convex, smooth surface. The synchondrosis spheno-occipitalis is clearly visible, as are the intraoccipital synchondroses. In class A, the synchodroses become seamlessly fused, the basioccipital acquires a rod-like appearance, and strong muscular tubercles develop.

The mastoid process from the squamosal adjoins the paracondylar process from the exo-occipital, and together form

Table 1 List of anatomical abbreviations used in the figures.

aC	canine alveolus	itf	infratemporal fossa	osqs	occipitosquamosa suture
aI1	first incisor alveolus	I3	third incisor	pal	palatine
aI2	second upper incisor alveolus	i1	first lower incisor	pet	petrosal
an	angle of mandible	i2	second lower incisor	pgf	postglenoid foramen
as	alisphenoid	i3	third lower incisor	pgp	postglenoid process
bcc	basicochlear commissure	ju	jugal	placs	palatine lacrimal suture
bo	basioccipital	lac	lacrimal	plp	palatine process of the premaxilla
bs	basisphenoid	lacf	lacrimal foramina	pls	palatine sulcus
c	lower canine	lacr	lambdoid crest (= nuchal crest)	pmx	premaxilla
cdc	condylar crest	lms	lacrimomaxillary suture	pop	postorbital process
cdp	condylar process	map	mastoid process	pp	paracondylar process
cf	carotid foramen	mapf	major palatine foramen	ppf	pterygopalatine fossa
cn	condylar notch	mas	mastoid	pps	pterygopalatine suture
cor	coronoid process	masy	mandibular symphysis	pr	promontorium
cp	canalicularis portion	md	mandibular diastema	prf	piriform fenestra
dI3	deciduous third incisive	mdf	mandibular foramen	ps	presphenoid
dP3	deciduous third premolar	mf	mental foramen	pt	pterygoid
dP4	deciduous fourth premolar	mfmx	masseteric fossa	P1	first premolar
eam	external acoustic meatus	mfp	maxilla frontal process	P2	second premolar
ect	ectotympanic	mn	mandibular notch	P3	third premolar
ef	ethmoidal foramen	mipf	minor palatine foramen	P4	fourth premolar
eo	exoccipital	mpf	maxillary process of the frontal	p1	first lower premolar
eoc	external occipital crest	mps	median palatine suture	p2	second lower premolar
eop	external occipital protuberance	msf	masseteric fossa	p3	third lower premolar
fls	frontolacrimal suture	mt	muscular tubercles	rac	rostral alar canal
fm	foramen magnum	mx	maxilla	sc	sagittal crest
fms	frontomaxillary suture	mxd	maxillary diastema	sfs	sphenofrontal suture
fns	frontonasal suture	mxt	maxillary tuber	smf	supramastoid foramen
fps	frontoparietal suture	M1	first molar	so	supraoccipital
fpz	frontal process of the zygomatic	M2	second molar	sosy	spheno-occipital synchondrosis
fr	frontal	M3	third molar	spf	sphenopalatine foramen
ftr	foramina for the temporal rami	m1	first lower molar	sps	sphenopalatine suture
gf	glenoid fossa	m2	second lower molar	sq	squamosal
hf	hypoglossal foramen	na	nasal	sqc	squamosal crest
if	incisive fissure	nmxs	nasomaxillary suture	sqs	squamosal suture
ifs	interfrontal suture	npf	nasal process of the frontal	ssqs	sphenosquamosal suture
imf	inframastoid foramen	oc	occipital condyle	tes	pterygosphenoid suture
ims	incisivomaxillary suture	ocr	orbital crest	thy	tympanohyoid
imxs	intermaxillary suture	of	orbital foramen	tps	transverse palatine suture
in	intercondyloid notch	oms	occipitomastoid suture	tzs	temporozygomatic suture
ins	internasal suture	ops	occipitoparietal suture	vo	vomer
iof	infraorbital foramen	os	orbitosphenoid	zls	zygomaticolacrimal suture
isy	intersphenoidalis synchondrosis	osf	ovale + spinosus foramen	zms	zygomaticomaxillary suture
I2	second incisor	pa	parietal	zpsq	zygomatic process of the squamosal
				zya	zygomatic arch

a thick, ventrally oriented process that occupies most of the space between the auditory meatus and the occipital condyle. Only a small mastoid exposure of the petrosal is apparent between these bones, pierced by the supramastoid and the inframastoid foramina (Fig. 6), which presumably transmit (in intracranial direction) the caudal meningeal artery and the caudal emissary vein, respectively (see Evans, 1993 and O'Brien et al. 2016). In class Y, the distal extent of the paracondylar process barely exceeds that of the mastoid process, and both processes are devoid of ridges or crests. In class A, the paracondylar process is approximately twice as long as the mastoid process, and it is highly variable in orientation, including directly ventral (e.g. CML 9830) and posteroventral (e.g. CML 9828). The mastoid process becomes sculptured with variable vertical ridges that continue dorsally to join the nuchal crest.

The elements of the auditory region do not exhibit major changes except for the texture of bone (from spongy to smooth) and the greater development of ridges and processes. However, the latter and other aspects are obscured by the significant variation across specimens, which preclude a precise determination of ontogenetic change. For

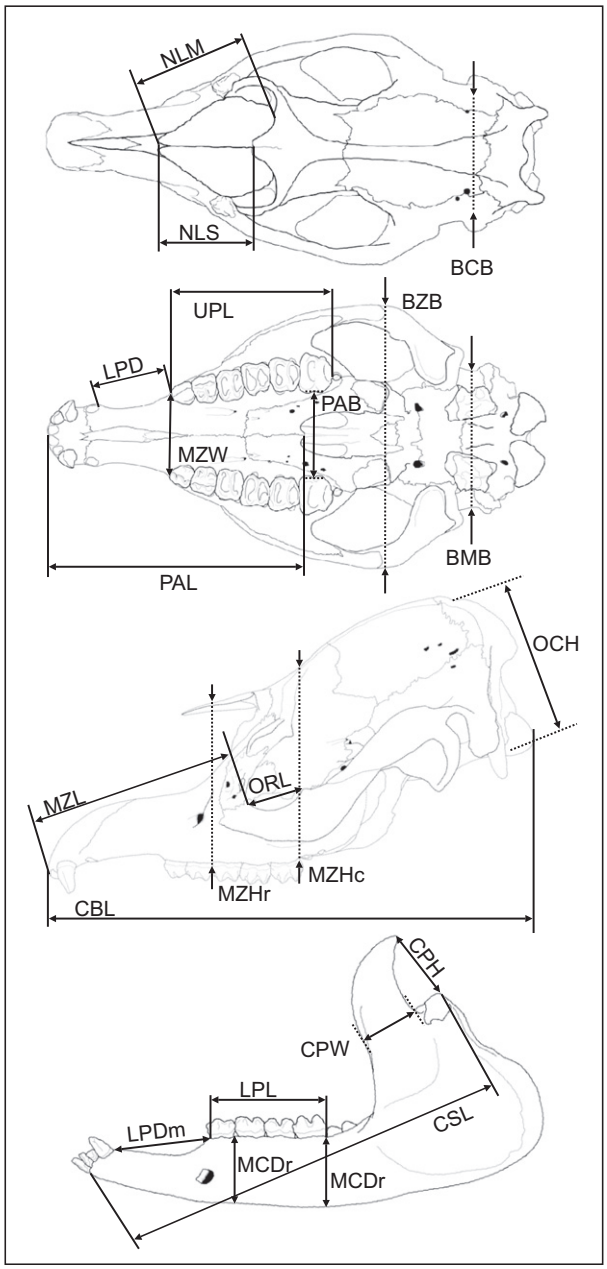

Fig. 12 Cranial measurements of *Tapirus terrestris* used in this study. BCB, braincase breadth; BMB, bimeatal breadth; BZB, bizygomatic breadth; CBL, condyle-basal length; CPH, coronoid process height; CPW, coronoid process width; CSL, condylo-symphysis length; LPD, diastema postcanine length; LPDm, mandibular diastema length; LPL, lower postcanine tooth row length; MCDc, mandibular corpus depth in last functional tooth; MCDr, mandibular corpus depth in the first functional tooth; MZHc, muzzle caudal height; MZHr, muzzle rostral height; MZL, muzzle length; MZW, muzzle width; NLM, nasal length maximum; NLS, nasal length on suture; OCH, occipital plate height; ORL, orbital length; PAB, palate breadth; PAL, palate length; UPL, upper postcanine tooth row length.

instance, the basicochlear commissure varies from absent (e.g. CML 9828) to strong (CML 9830). A short, cup-shaped ectotympanic is preserved in right side of class Y (AMNH 202838; Fig. 7); this element is missing in the remainder of our sample and therefore no ontogenetic comparisons were possible. Likely the petrosal-ectotympanic articulation is weak and therefore detachment and loss of the ectotympanic is frequent in museum specimens.

A tympanohyoid is well developed already in class Y. The preserved right ectotympanic of this specimen (AMNH 202838; Fig. 7) caudally abuts the corresponding tympanohyoid, which shows a platform-like shape in ventral view, as in full and old adults (Fig. 7).

Mandible. The main ontogenetic changes observed during the ontogeny of the mandible are summarized in Table 4. The mandible is a gracile bone in class Y and a fairly robust one in class A, but the overall adult shape is faithfully represented already in the very young juvenile. One of the most important changes observed were the rostrocaudal elongation of the diastema, absent in class Y (Figs 8 and 9) and extended to occupy almost one-fourth of the old adult mandible (see quantitative analysis below). The stable position of the lateral mental foramen, fixed between one-third and one-fourth of the mandibular length in both class Y and class A, indicates that the remodeling of the mandibular body occurred chiefly, if not exclusively, on the dental surface, thus originating the diastema as the mandible added dental elements. The muscle orbicularis oris originates over the mandibular diastema and surrounds the mouth to form the ventrolateral portion of the proboscis (Witmer et al. 1999). The surface of attachment of the strong masseter muscle is neatly marked in class A but is poorly defined in class Y. The attachment area of the pterygoid muscle, in the medial surface of the angular process, increased its concavity and rugosity toward the condition in class A.

Cranial joints. Changes in the condition of cranial joints are depicted in Fig. 11. Thirteen joints exhibited no ontogenetic change and these were mostly squamous sutures of the cranium; seven plane sutures became serrated, of which all but the occipitomastoid were rostral sutures; only one serrated suture, the median palatine suture, fused during development; all four median sutures (interincisive, internasal, interfrontal and sagittal), originally plain, fused toward adulthood; four squamous sutures fused, two associated with the pterygoid bone and two transverse sutures of the cranial vault (frontoparietal and occipitoparietal); and two plane sutures that become squamous are associated with the palatine bone. Regarding synchondroses, in all cases (s. intersphenoidalis, s. spheno-occipitalis, s. intraoccipitalis basilateralis, and s. intraoccipitalis occipitolateralis) changed from open or partially open to fused with age (Fig. 11). From the previous tally, it is clear that changes in the condition of sutures are largely congruent within skull regions or planes (e.g. all median sutures fused), and are diverse across the skull. In addition, we noted two main

Table 2 List of morphological changes detected in the rostral bones in a comparison of age class of specimens of *Tapirus terrestris*, indicating the figure where the character is observed.

Characters	Figures	Class Y	Class J	Class A
1. PREMAXILLA	2, 3, 5, 9	Short and straight	Longer and rostroventrally curved	Rostrocaudally elongated, rostroventrally curved and transversely expands
Dorsal accessory foramina in premaxilla	3	Absent	Present with irregular distribution	Many tiny foramina in the rostral portion
Ventral accessory foramina in premaxilla	1, 2	Absent	Many tiny foramina, most caudally present in each incisor	Tiny foramina
Palatine process of the premaxilla	1, 2	Slightly concave	Concave	Concave
2. MAXILLA	5, 10	Short maxillary diastemata	Large maxillary diastemata	Large maxillary diastemata
Infraorbital foramen	5, 10	Varies from rounded to slightly dorsoventrally elongated	Slightly dorsoventrally elongated	Dorsoventrally elongated
Frontal process of the maxilla	1, 3	Slightly concave and caudally elongated relying on the frontal bone	Concave	Concave
Zygomatic process of the maxilla	5, 10	Short	Laterally extended. In some, it contacts with the squamosal zygomatic process	Laterally extended. In some, it contacts with the squamosal zygomatic process
Maxillary foramen		Rounded shape	More dorsoventrally elongated	Dorsolaterally elongated or the base is expanding with an almost triangular shape
Masseteric fossa (ventral view of the maxilla)	1, 2	Rostrocaudally elongated. Poorly marked	Rostrocaudally elongated. Very evident	Rostrocaudally elongated. Very evident
Major palatine foramen	1, 2	With a delicate palatine sulcus rostrally elongated but not exceeding the premolars	Strong sulcus extended to incisive fissure	Strong sulcus extended to incisive fissure
3. NASAL	3, 4, 10	Short. The left and right portion of the nasal bone form a triangular structure	With a caudally located bilobate base	Large. Slightly pentagonal form with expanded lateral margin
4. JUGAL (= Zygomatic)	5, 10	Thin. Caudal half is dorsoventrally slightly high	Wide. Caudal half is dorsoventrally high	Wide and robust. Caudal half is dorsoventrally high
5. LACRIMAL	5, 10	Both foramina are open towards the caudal face.	Lower lacrimal foramen open in the rostral face. The major dorsal foramen is larger.	Both foramina open towards the caudal face. The major dorsal foramen is larger.
6. PALATINE	1, 2	Horizontal lamina is slightly concave	Concavity is further accented	Concavity is further accented
Pterygopalatine fossa	5, 10	Concave with smooth surface	More concave and irregular surface	Concave and more irregular surface
Accessory foramina of the palatine	1, 2	Few small foramina. and rostrocaudally elongated	Many foramina with irregular distribution and size	Many tiny foramina and the same size or smaller than the palatine foramen
7. PTERYGOID	1, 2	Short lamina. With a little projection in the upper end like a short and rounded tubercle	Larger lamina. The base is caudally projected and in contact with presphenoid and basisphenoid bones	Larger lamina. Pterygoid fused to palatine

types of changes, one in the direction of strengthening of the joint (plane to serrate, serrate to fuse), and another in the direction of large bone overlap (plane to squamous). The great majority of changes were of the former type, indicating an increased strengthening and rigidity of the skull along the ontogeny, which likely aids in withstanding

Table 3 List of morphological changes detected in the cranial bones in a comparison of age class of specimens of *Tapirus terrestris*, indicating the figure where the character is observed.

Characters	Figure	Class Y	Class J	Class A
1. FRONTAL	3	Caudally broad	Caudally narrow	Caudally narrow
Postorbital process of the frontal	5, 10	Poorly developed	More developed	Very developed
Ethmoidal foramen	5, 10	Circular	Circular to dorsoventrally elongated	Dorsoventrally elongated
Maxillary process of the frontal	4, 5, 10	Smooth and thin surface Broad and laterally extended	Slightly porous surface. In later specimen, the surface is very irregular	Strong and sculptured surface. It is thick, medially concave and laterally convex
Nasal process of the frontal	4, 5, 10	Triangular extension with smooth surface	Triangular extension with porous surface	Triangular extension with porous surface
Orbit	5, 10	Circular	Oval	Oval
2. PARIETAL	3, 5, 10	Skull with globular-shape. Sagittalis suture flat	Dorsally elevated. Sagittal suture is elevated forming a crest.	Convex lateral wall. Midline slightly concave and elevated in crest.
3. SPHENOID COMPLEX				
Presphenoid	1, 2	Fused to orbitosphenoid and not to the basisphenoid. Poorly relying on the vomer	Is overlapped by caudal expansion of the vomer	Is overlapped by caudal expansion of the vomer. Lateral and caudally fused to basisphenoid
Basisphenoid	1, 2	In AMNH 202838, smooth and flat surface. Rostral half with trapezoidal-shape and caudally narrow forming a central trunk	With concave surface on the midline. Robust bone	The concave surface on the midline. Robust bone The trunk caudally elongated
Alisphenoid	1, 2	The orbital fenestral, pterygoid canal and rostral alar foramen are inside the same fossa. Pterygoid canal rounded or dorsoventrally elongated	Foramina openings retarded in the fossa	Foramina openings are caudally retarded, making it difficult to determine its shape
4. SQUAMOSAL	5, 10	Lateral surface of the process is flat	Lateral surface of the process is concave	Lateral surface of the process is concave
Glenoid fossa	1, 2	Not deep. With smooth surface and slightly concave	Deep	Very deep
Postglenoid process	1, 10	Thin. Slightly ventrorostrally curved	Ventrally elongated and ventrorostrally curved	Strong. Rostrally curved with irregular surface
Mastoid process	5, 10	Smooth surface	Irregular surface with excrescences	Irregular surface with excrescences
Zygomatic process of the squamosal	5, 10	Thin	Strong with a concave surface	Strong with a concave surface
5. OCCIPITAL COMPLEX				
Supraoccipital	3, 6	Absent nuchal crest. In caudal view left and right crests are two soft arches	More marked nuchal crest.	Roughly marked and caudally expanded nuchal crest.
External occipital crest	6	Poorly developed. Small protuberance extending from the nuchal crest to the foramen magnum	Developed. Wide and shorter	Very developed. Wide and shorter
Basioccipital	1, 2	Straight to slightly concave caudal edge	Concave caudal edge. Rostrocaudally elongated	Concave caudal edge. Rostrocaudally elongated
MASTOID	6	Smooth surface	Irregular surface	Irregular surface
Supramastoid foramen	6	Rounded	Rounded and slightly dorsoventrally elongated	Dorsoventrally elongated (Faint)
Inframastoid foramen	6	Rostrocaudally elongated	Rostrocaudally elongated	Rostrocaudally elongated

increased loads generated by mastication of fibrous food (Rafferty et al. 2003). The interdigitations of serrated sutures increase the contact area of the adjoining bone surfaces, and may increase the number of collagen fibers in the suture (see Jaslow, 1990; Rafferty et al. 1999; Herring & Rafferty, 2000; and Sun et al. 2004; Herring, 2008). Finally,

the mandibular symphysis fuses early as in other ungulates and higher primates (see Rafferty et al. 2003).

Quantitative analysis: cranial allometry in *Tapirus*

Results of our multivariate analysis of allometry are shown in Table 5. In *T. terrestris*, the observed allometric trends were isometric in five of 23 variables, or *ca*. 22% (CBL, MCDr, MZHc, MZL, PAB). In turn, nine variables (or *ca.* 39%) were 'positively' allometric (CPW, LPD, LPDm, LPL, MCDc, NLS, NLM, PAL, UPL), and the other nine variables (another ca. 39%) were 'negative' (BCB, BMB, BZB, CSL, CPH, MZW, MZHr, OCH, ORL).

In *T. indicus*, the observed allometric trends were isometric in four of 23 variables, or *ca.* 17% (CSL, BZB, NLM, PAB). We detected seven variables, or transmit 30%, with 'positive' allometry (CPH, CPW, MZL, MZHc, LPL, PAL, UPL) and 12 variables, or transmit 52%, with negative allometry (BCB, BMB, CBL, LPD, LPDm, MCDc, MCDr, MZHr, MZW, NLS, OCH, ORL).

A depiction of comparative skull allometry of the two species is presented in Fig. 13. *Tapirus indicus* and *T. terrestris* shared 11 growth allometric trends, or transmit 48% of variables. Of the common set, six variables (BCB, BMB, MZHr, MZW, OCH, ORL) were negative allometric; four (CPW, LPL, PAL, UPL) were positive allometric and only one (PAB) was isometric (Fig. 13, Table 5). Of the remaining variables, seven showed partially similar trends (i.e. positive or negative trend for one species and isometric for other species; BZB, CBL, CSL, MCDr, MZHc, MZL, NLM); and five showed completely different trends (i.e. opposite signs: CPH, LPD, LPDm, MCDc, NLS) (Fig. 13, Table 5). Two of these variables (MZL, CBL) were statistically allometric in one species and isometric in the other, their actual intervals overlapped, meaning that they did not differ in evolutionary terms (i.e. they would be reconstructed as sharing an interval in their common hypothetical ancestor; see Giannini, 2014, for details).

Skull growth in the species with the largest sample, *T. terrestris*, can be quantitatively described as follows. Longitudinal rostral components grew with positive allometry, specifically length of nasals (NLrS), palate (PAL), upper and lower toothrow and diastemata (UPL, LPL, LPD, and LPDm, respectively), whereas transverse and vertical components, specifically width of palate (PAB) and muzzle (MZW), and anterior muzzle height (MZHr) and anterior mandible height (MCDr), grew isometrically, or 'negatively', thus composing a growth pattern of tapering, narrowing rostrum toward adulthood. In addition, this developmental pattern is also evident on a qualitative basis (see above) and matches very well the browsing habits of adult tapirs (in general, browsing ungulates exhibit significantly narrow muzzles as compared with grazing counterparts; see Owen-Smith, 1982). All neurocranial components exhibited 'negative' allometry as expected, but gradual differences were important; specifically, the least 'negatively' allometric component was the height of the occiput (OCH), which involves crest development in the South American tapir (but see below).

The second species analyzed, *T. indicus*, showed wider confidence intervals in several variables compared with *T. terrestris* (e.g. NLS, LPD, LPDm), almost certainly reflecting the smaller sample size for the species ($n = 25$ in *T. indicus*, $n = 46$ in *T. terrestris*). The Malayan tapir showed a similar pattern of skull growth to the South American tapir described above, but with noticeable differences that are unlikely to be due to sample size differences. The upper toothrow length (UPL) was the most 'positive' trend in the

Table 4 List of morphological changes detected in the mandible in a comparison of age class of specimens of *Tapirus terrestris*, indicating the figure where the character is observed.

Characters	Figure	Class Y	Class J	Class A
Diastema	8, 9	Short	Rostrocaudally elongated and becoming narrow in the development, forming a constriction	Rostrocaudally elongated
Mental foramen	9	In the very young juvenile, it is round. In late specimens, it is elongated	Predominantly elongated	Predominantly elongated
Masseteric fossa	9	Faint	Marked	Marked
Angle of the mandible	9	With faint edge	With marked edge	With marked edge
Condyle process	8, 9	Like a cross bar with porous surface and sagittally convex. Dorsomedially inclined. Laterally poorly developed	Like a cross bar with porous surface and sagittally convex Laterally developed	Like a cross bar with porous surface and sagittally convex Laterally developed
Fossa in the medial surface of the ramus		Smooth surface	Deep surface with dorsocaudal fingerings	Caudal and ventral border medially curved

Table 5 Results of the multivariate analysis of cranial in *Tapirus indicus* (Ti; n = 25) and *Tapirus terrestris* (Tt; n = 46).

		Untrimmed					Trimmed				
Var	sp	Unbiased coeff.	Bias	95% CI	Departure	Growth trend	Unbiased coefficient	Bias	95% CI	Departure	Growth trend
Cranium											
CBL	Ti	0.225	−1.44E-02	0.189–0.26	0.017	iso	0.196	3.66E-04	0.185–0.207	−0.013	−
	Tt	0.216	−8.87E-04	0.2–0.23	0.007	iso	0.209	2.85E-03	0.203–0.214	0	iso
PAL	Ti	0.276	−1.67E-02	0.235–0.32	0.068	+	0.247	−2.32E-03	0.232–0.263	0.039	+
	Tt	0.229	−1.15E-04	0.214–0.24	0.02	+	0.223	2.80E-03	0.215–0.231	0.014	+
PAB	Ti	0.303	−3.32E-02	0.179–0.43	0.095	iso	0.201	1.80E-02	0.173–0.229	−0.007	iso
	Tt	0.199	1.36E-03	0.166–0.23	−0.009	iso	0.2	1.23E-03	0.178–0.221	−0.009	iso
MZW	Ti	0.244	−4.75E-02	0.054–0.43	0.036	iso	0.092	2.87E-02	0.05–0.134	−0.117	−
	Tt	0.098	1.24E-03	0.038–0.16	−0.111	−	0.096	2.26E-03	0.078–0.113	−0.113	−
MZL	Ti	0.262	−1.58E-02	0.222–0.3	0.054	+	0.231	−4.98E-04	0.218–0.245	0.023	+
	Tt	0.219	−3.30E-04	0.2–0.24	0.011	iso	0.212	3.44E-03	0.2–0.223	0.003	iso
NLS	Ti	0.127	−1.94E-02	−0.01–0.27	−0.082	iso	0.077	5.40E-03	0.007–0.147	−0.131	−
	Tt	0.261	−1.09E-04	0.219–0.3	0.053	+	0.287	−1.31E-02	0.265–0.309	0.079	+
NLM	Ti	0.201	1.18E-02	0.104–0.3	−0.007	iso	0.236	−5.68E-03	0.182–0.29	0.027	iso
	Tt	0.245	−4.03E-04	0.217–0.27	0.036	+	0.254	−4.96E-03	0.239–0.269	0.045	+
OCH	Ti	0.193	−2.16E-02	0.114–0.27	−0.016	iso	0.133	8.61E-03	0.115–0.15	−0.076	−
	Tt	0.194	−1.41E-03	0.177–0.21	−0.014	iso	0.185	2.95E-03	0.175–0.195	−0.023	−
LPD	Ti	0.218	−4.25E-02	−0.03–0.46	0.01	iso	0.027	5.31E-02	−0.028–0.082	−0.181	−
	Tt	0.248	−1.10E-03	0.217–0.28	0.039	+	0.248	−1.44E-03	0.228–0.269	0.04	+
UPL	Ti	0.294	3.46E-02	0.096–0.49	0.086	iso	0.453	−4.50E-02	0.413–0.494	0.245	+
	Tt	0.262	2.25E-03	0.226–0.3	0.053	+	0.272	−3.17E-03	0.249–0.296	0.064	+
MZHr	Ti	0.222	−2.71E-02	0.124–0.32	0.013	iso	0.139	1.45E-02	0.126–0.152	−0.07	−
	Tt	0.154	−4.37E-04	0.145–0.16	−0.054	−	0.154	−1.18E-04	0.147–0.16	−0.055	−
MZHc	Ti	0.282	−2.11E-02	0.217–0.35	0.073	+	0.234	2.65E-03	0.214–0.255	0.026	+
	Tt	0.205	1.13E-03	0.185–0.22	−0.004	iso	0.208	−3.89E-04	0.193–0.222	−0.001	iso
ORL	Ti	0.113	3.14E-03	0.05–0.18	−0.095	−	0.124	−1.99E-03	0.084–0.164	−0.085	−
	Tt	0.097	−3.56E-05	0.08–0.12	−0.111	−	0.099	−7.88E-04	0.085–0.113	−0.11	−
BCB	Ti	0.024	9.02E-03	−0.05–0.1	−0.185	−	0.014	1.39E-02	−0.022–0.05	−0.194	−
	Tt	0.064	−1.18E-03	0.05–0.08	−0.145	−	0.064	−1.33E-03	0.054–0.074	−0.144	−
BMB	Ti	0.151	−1.38E-02	0.098–0.21	−0.057	−	0.119	2.45E-03	0.108–0.13	−0.09	−
	Tt	0.11	−8.63E-04	0.096–0.12	−0.099	−	0.104	2.15E-03	0.096–0.112	−0.105	−
BZB	Ti	0.223	−1.20E-02	0.185–0.26	0.014	iso	0.203	−2.22E-03	0.183–0.224	−0.005	iso
	Tt	0.17	−1.37E-04	0.155–0.18	−0.039	−	0.172	−1.41E-03	0.163–0.181	−0.036	−
Mandible											
CSL	Ti	0.215	−7.47E-03	0.203–0.23	0.006	iso	0.212	−6.08E-03	0.203–0.221	0.004	iso
	Tt	0.193	−2.59E-04	0.185–0.2	−0.015	−	0.193	−2.51E-04	0.188–0.199	−0.015	−
LPDm	Ti	0.251	−5.05E-02	0.04–0.46	0.043	iso	0.088	3.13E-02	0.034–0.141	−0.121	−
	Tt	0.335	−5.41E-03	0.287–0.38	0.127	+	0.315	4.85E-03	0.284–.346	0.106	+
LPL	Ti	0.267	5.20E-02	−0.02–0.55	0.058	iso	0.498	−6.37E-02	0.454–0.542	0.289	+
	Tt	0.244	2.98E-03	0.211–0.28	0.036	+	0.257	−3.27E-03	0.24–0.274	0.048	+
MCDr	Ti	0.18	−2.88E-02	0.066–0.29	−0.028	iso	0.09	1.62E-02	0.066–0.115	−0.118	−
	Tt	0.198	−4.81E-04	0.177–0.22	−0.01	iso	0.202	−2.33E-03	0.188–0.215	−0.007	iso
MCDc	Ti	0.286	−3.55E-02	0.149–0.42	0.077	iso	0.176	1.94E-02	0.146–0.207	−0.032	−
	Tt	0.213	2.54E-04	0.197–0.23	0.004	iso	0.219	−2.79E-03	0.21–0.227	0.01	+
CPH	Ti	0.32	−2.96E-02	0.232–0.41	0.112	+	0.257	1.81E-03	0.226–0.288	0.049	+
	Tt	0.193	−1.14E-03	0.16–0.23	−0.016	iso	0.183	3.63E-03	0.164–0.203	−0.025	−
CPW	Ti	0.261	−1.32E-02	0.227–0.29	0.052	+	0.249	−7.61E-03	0.229–0.27	0.041	+
	Tt	0.257	−3.92E-03	0.224–0.29	0.049	+	0.24	4.53E-03	0.222–0.258	0.032	+

Variable abbreviations as in Fig. 12.

Unbiased coefficient, value generated by first-order jackknife resampling; Bias, difference between the unbiased and observed coefficients; 95% CI, jackknifed 95% confidence interval (CI) – allometric variables are those whose CIs exclude the expected value under isometry (0.208). Departure, subtraction of expected value under isometry from the unbiased coefficient; Growth trend, allometric trend of each variable. iso, isometry; −, negative allometry; +, positive allometry; Var, variables.

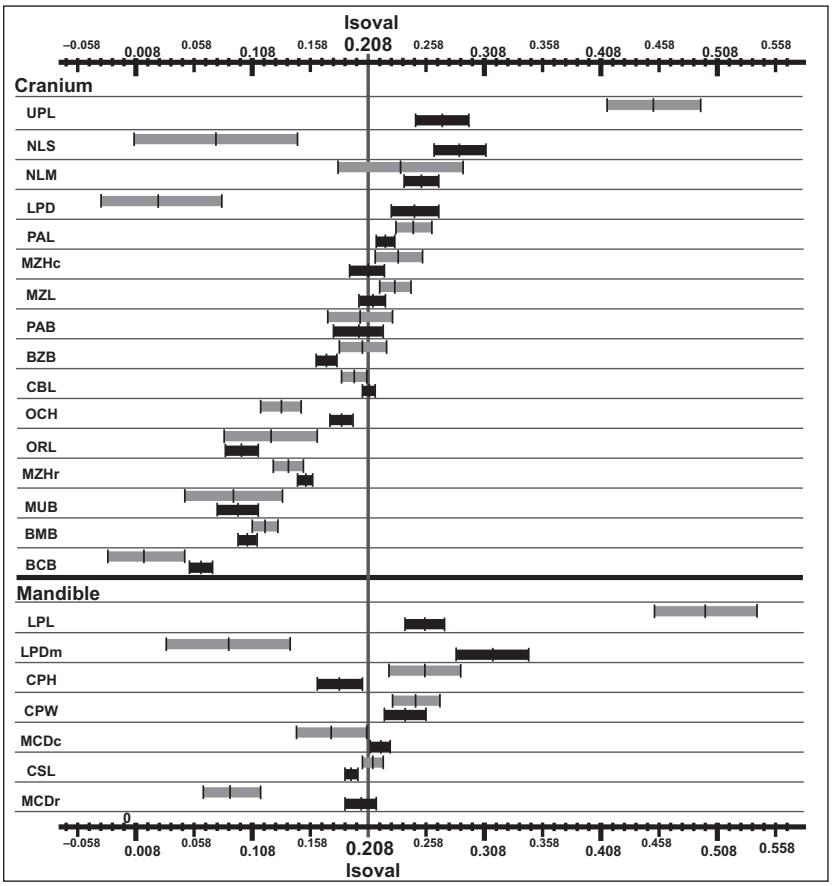

Fig. 13 Distribution of confidence intervals of each species with respect to the isometric value (0.208). Black color lines are *Tapirus terrestris*; gray color lines are *T. indicus*. Variable abbreviations as in Fig. 12.

whole sample, and the multivariate coefficient of allometry was considerably larger in *T. indicus* (unbiased estimate at 0.453 as compared with 0.272 in *T. terrestris*; Fig. 13). The reverse pattern, as expected, was observed in the length of the upper diastema (LPD), and this was replicated for both variables in the mandible (i.e. accelerated rate of growth in the toothrow, decelerated rate in the diastema on both upper and lower toothrow; Fig. 13). The nasal length (NLS) also exhibited a contrasting pattern between species, with strongly 'negative' allometry in *T. indicus*, which we interpret not as a nasal developmental difference *per se* but as a result of the increasing overlap of the frontal over the nasal (pattern not observed in the frontonasal suture in *T. terrestris*; see above). The muzzle length (MZL) and posterior muzzle height (MZHc) grew relatively faster than the skull as a whole in *T. indicus* than in *T. terrestris* (Fig. 13), which likely generated space for a larger proboscis in the former. The rate of growth also differed in the coronoid process (CPH, greater in *T. indicus*), the height of mandible (MCDc and MCDr, greater in *T. terrestris*) and, most interestingly, the height of the occipital plate (OCH), which in spite of being 'negatively' allometric in both species, grew at a faster pace in *T. terrestris* (Fig. 13), reflecting the presence of tall crests in the occiput. Overall, these results indicate subtle differences between species in modeling of the masticatory apparatus that were detectable with our quantitative analysis and certainly reflect biomechanical differences, most obviously associated to the action of the temporalis muscle.

Conclusion

Skull growth in *Tapirus terrestris* is relatively conservative along postnatal ontogeny, but quantitative analysis revealed changes that do occur during ontogeny and involve chiefly the masticatory apparatus. The muzzle elongated and narrowed significantly, accompanied by a proportional decrease in size of the anterior dentition, whereas neurocranial components exhibited varying degrees of 'negative' allometry. Overall these changes depict the morphological development of a browsing ungulate and its ability to select specific plant material such as leaves (see Owen-Smith, 1982). But, in addition, in the tapir the proboscis takes over part of the food-gathering function, which in other browsers rests entirely in the anterior dentition. On the basis of qualitative analysis, development of a flexible proboscis is shown here to alter the surface and structure of several rostral bones, particularly those areas that contribute to the formation of the meatal diverticulum and those surfaces that provide the origin for the complex, highly modified rostral musculature of the tapir. The nasal region changes to accommodate the

meatal diverticulum by means of increased depth of its containing fossa and development of ridges and tuberosities for origin of the complex ocular and proboscis musculature. The increasing importance of the postcanine dentition with age is reflected in ontogenetic changes observed in our tapir skull series. Fitting the large molars in the upper toothrow as they emerge in rostrocaudal sequence causes a major remodeling of this area and the largest landmark displacements in the growing skull (maxillary tuber and orbital floor). This further contributes to the browsing diet by providing the grinding surface for processing a volume of foliage required to nurture a mammal the size of the tapir. Also the sagittal and nuchal crests grow proportionally more in *T. terrestris* than in any other tapir species. Increase in the space available for the temporalis muscle is reflected in both development of the sagittal crest and the postorbital constriction. More subtle changes are also registered in the elongation of the skull base. Joints change dramatically across the ontogeny; most changes involve a strengthening of the joint and an increase in general rigidity of the skull. These changes are consistent in type within a given region of the skull, but are diverse across regions of the skull. The overall pattern of the postnatal ontogeny of *T. terrestris* reflects the gradual acquisition of a browsing habit and development of a highly movable, short proboscis. We established a basis of comparison with the Malayan tapir, *T. indicus*, which shows that most patterns seen in the focal species of this study are shared across the group, but we also showed quantitative grow differences in variables of the masticatory apparatus that allow a clear distinction between these two species.

Acknowledgements

We thank David Flores and Sergio Lucero (MACN, Bernardino Rivadavia, Buenos Aires, Argentina); Rubén Bárquez and Mónica Díaz (CML, Tucumán, Argentina); Enrique González and Yennifer Hernandez (MNHN, Montevideo, Uruguay); Bruce Patterson and Bill Stanley (FMNH, Chicago, IL, USA); Darrin P. Lunde (USNM, Washington DC, USA) and Eileen Westwig (AMNH, New York, NY, USA) for granting access to installations and specimens under their care. We thank Paul Velazco and Damian Arancibia for their impartial collaboration. Thanks to Miriam Morales for help us in the measurements. We also thank two anonymous reviewers whose comments significantly improved the quality of this manuscript. This study was partially supported by the Consejo Nacional de Investigaciones Científicas y Técnicas (CONICET) to S.R.M. and Grant FONCyT PICT 2008-1798 to N.P.G.

Author contributions

S.R.M. and N.P.G. designed the study and interpreted the data. S.R.M collected the data, wrote the first version of manuscript, and made the figures and tables. N.P.G. finished the writing.

Conflict of interest

The authors declare no conflict of interest.

References

Abdala F, Flores DA, Giannini NP (2001) Postweaning ontogeny of the skull of *Didelphis albiventris*. *J Mammal* **82**(1), 190–200.

Ayala G (2003) Monitoreo de *Tapirus terrestris* en el Izozog (Cerro Cortado) mediante el uso de telemetría como base para un plan de conservación. Master's thesis, Institute of Ecology, Universidad Mayor de San Andrés, La Paz, Bolivia.

Beddard FE (1909) Contributions to the anatomy of certain ungulata, including *Tapirus*, *Hyrax*, and *Antilocapra*. Proc Zool Soc Lond **79**, 160–197.

Bell RHV (1969) The use of the herbaceous layer by grazing ungulates in the Serengeti National Park, Tanzania. PhD thesis, University of Manchester.

Bell RHV (1970) The use of the herb layer by grazing ungulates in the Serengeti. In: *Animal Populations in Relation to Their Food Resources* (ed. Watson A), pp. 111–123. Tenth Symposium of the British Ecology Society. Oxford: Blackwell Scientific Publications.

Bodmer R (1990) Fruit match size and frugivory in the lowland tapir (*Tapirus terrestris*). *J Zool* **222**(1), 121–128.

Bodmer R, Brooks DM (1997) Evaluación del estado y plan de acción del tapir de tierra baja (*Tapirus terrestris*). In: *Tapirs Status Survey and Conservation Action Plan* (eds Brooks DM, Rodmer RE, Matola S). Gland, Switzerland and Cambridge, UK: IUCN/SSC Tapir Specialist Group, IUCN.

de Bustos S, Chalukian S, Lizárraga L, et al. (2004) El tapir como arquitecto de bosques secundarios: su impacto sobre renovales leñosos en el Parque Nacional El Rey. II Reunión Binacional de Ecología, Mendoza.

Cassini GH, Flores DA, Vizcaíno SF (2012) Postnatal ontogenetic scaling of Nesodontine (Notoungulata, Toxodontidae) cranial morphology. *Acta Zool* **93**, 249–259.

Cassini GH, Flores DA, Vizcaíno SF (2015) Postnatal ontogenetic scaling of Pampas Deer (*Ozotoceros bezoarticus celer*: Cervidae) cranial morphology. *Mammalia* **79**(1), 69–79.

Cozzuol MA, Clozato CL, Holanda EC, et al. (2013) A new species of tapir from the Amazon. *J Mammal* **94**(6), 1331–1345.

Evans HE (1993) *Miller's Anatomy of the Dog*. 3rd edn. Philadelphia: Saunders.

Flores DA, Giannini N, Abdala F (2006) Comparative postnatal ontogeny of the skull in the australidelphian metatherian *Dasyurus albopunctatus* (Marsupialia: Dasyuromorpha: Dasyuridae). *J Morphol* **267**(4), 426–440.

Flores DA, Abdala F, Giannini NP (2013) Post-weaning cranial ontogeny in two bandicoots (Mammalia, Peramelomorphia, Peramelidae) and comparison with carnivorous marsupials. *Zoology* **116**, 374–384.

Giannini NP (2014) Quantitative Developmental Data in a Phylogenetic Framework. *J Exp Zool (Mol. Dev. Evol.)* **9999**, 1–9.

Giannini N, Abdala F, Flores DA (2004) Comparative postnatal ontogeny of the skull in *Dromiciops gliroides* (Marsupialia: Microbiotheriidae). *Am Mus Novi* **3460**, 1–17.

Giannini NP, Segura V, Giannini MI, et al. (2010) A quantitative approach to the cranial ontogeny of the puma. *Mamm*

Biol **75**(6), 547–554. https://doi.org/10.1016/j.mambio.2009.08.001.

Gibson ML (2011) Population Structure Based on Age-Class Distribution of *Tapirus polkensis* from the Gray Fossil Site Tennessee. Electronic Theses and Dissertations. Paper 1267. http://dc.etsu.edu/etd/1267

Gould SJ (1977) *Ontogeny and phylogeny*. Cambridge, Mass: Harvard University Press.

Gwynne MD, Bell RHV (1968) Selection of vegetation components by grazing ungulates in the Serengeti National Park. *Nature* **220**, 390–393.

Hatcher JB (1896) Recent and fossil tapirs. *Am J Sci* **3**, 161–180.

Herring SW (2008) Mechanical influences on suture development and patency. *Craniofacial Sutures***12**, 41–56.

Herring SW, Rafferty KL (2000) Cranial and facial sutures: functional loading in relation to growth and morphology. Biological mechanisms of tooth eruption, resorption and replacement by implants. Boston: Harvard Society for Advanced Orthodontics 269–276.

Hershkovitz P (1954) Mammals of Northern Colombia, preliminary report no. 7: Tapirs (gen. *Tapirus*) with a systematic review of American species. Proc. US Natl Museum **103**, 465–496.

Holanda E (2007). Os Tapiridae (Mammalia, Perissodactyla) do Pleistoceno Superior do estado de Rondônia, Brasil. Dissertação (Mestrado). Universidade Federal do Rio Grande do Sul. Instituto de Geociências. Programa de Pós-Graduação em Geociências. Porto Alegre, RS - BR.

Holbrook LT (2002) The unusual development of the sagittal crest in the Brazilian tapir (*Tapirus terrestris*). *J Zool Soc Lond* **256**, 215–219.

Huxley JS (1932) *Problems of Relative Growth*. London: Methuen & Co., Ltd..

Janis CM (1995) Correlation between craniofacial morphology and feeding behavior in ungulates: reciprocal illumination between living and fossil taxa. In: *Functional Morphology in Vertebrate Paleontology* (ed. Thomason JJ), pp. 76–98. Cambridge: Cambridge University Press.

Janis CM, Ehrhardt D (1988) Correlation of relative muzzle width and relative incisor width with dietary preference in ungulates. *Zool J Linn Soc* **92**(3), 267–284.

Jarman P (1974) The social organization of antelope in relation to their ecology. *Behaviour* **48**(1), 215–267.

Jaslow CR (1990) Mechanical properties of cranial sutures. *J Biomech* **23**(4), 313–321.

Jolicoeur P (1963) The multivariate generalization of the allometry equation. *Biometrics* **9**, 497–499.

Kemp TS (2005) *The Origin and Evolution of Mammals*. New York, United States: Oxford University Press.

Klingenberg CP (1996) Multivariate allometry. *Nato Asi Series a Life Sci* **284**, 23–50.

Klingenberg CP, Zimmermann M (1992) Static, ontogenetic, and evolutionary allometry: a multivariate comparison in nine species of water striders. *Am Nat* **140**(4), 601–620.

Linnaeus C (1758) *Systema naturae per regna tria naturae, secundum classes, ordines, genera, species, cum characteribus, differentiis, synomymis, locis*. 10th edn. Vol. **1**, pp. 1–824, Stockholm: Laurentii Salvii.

Maffei L (2003) The Age Structure of Tapirs (*Tapirus terrestris*) in the Chaco. *Tapir Conservation* **12**, 18–19.

Manly BFJ (1997) *Randomization, Bootstrap, and Monte Carlo Methods in Biology*. 2nd edn. London: Chapman and Hall.

Milewski AV, Dierenfeld ES (2013) Structural and functional comparison of the proboscis between tapirs and other extant and extinct vertebrates. *Integr Zool* **8**(1), 84–94.

Mitteroecker P, Gunz P, Windhager S, et al. (2013) A brief review of shape, form, and allometry in geometric morphometrics, with applications to human facial morphology. *Hystrix It J Mamm* **24**(1), 59–66.

Mosimann JE (1970) Size allometry: size and shape variables with characterizations of the lognormal and generalized gamma distributions. *JASA* **65**(330), 930–945.

Naveda A, deThoisy B, Richard-Hansen C, et al. (2008) *Tapirus terrestris*. The IUCN Red List of Threatened Species: e.T21474A9285933. https://doi.org/10.2305/iucn.uk.2008.rlts.t21474a9285933.en (accessed 14 February 2017).

Norman JE, Ashley MV (2000) Phylogenetics of Perissodactyla and Test of the Molecular Clock. *J Mol Evol* **50**, 11–21.

O'Brien HD, Gignac PM, Hieronymus TL, et al. (2016) A comparison of postnatal arterial patterns in a growth series of giraffe (Artiodactyla: *Giraffa camelopardalis*). *PeerJ* **4**, e1696.

Owen-Smith N (1982) Factors influencing the consumption of plant products by large herbivores. In: *The Ecology of Tropical Savannas*. (eds Huntley BJ, Walker BH), pp.359–404, Berlin: Springer-Verlag.

Padilla M, Dowler RC (1994) *Tapirus terrestris.* Mamm Species **481**, 1–8.

Parker WN (1882) On some Points in the Anatomy of the Indian Tapir (*Tapirus indicus*)Proc Zool Soc London ,768–777.

Paulli S (1900) Über die Pneumaticität des Schädels bei den Säugethieren. II. Über die morphologie des Siebbens und die der Pneumaticität bei den Ungulaten und Proboscіden. *Morphol Jahrb* **28**, 179–251.

Quenouille MH (1956) Notes on bias in estimation. *Biometrika* **43**, 353–360. https://doi.org/10.2307/2332914.

Radinsky LB (1965) Evolution of the tapiroid skeleton from *Heptodon* to *Tapirus*. *Bull Mus Comp Zool* **134**, 69–106.

Radinsky LB (1966) The adaptive radiation of the phenacodontid condylarths and the origin of the Perissodactyla. *Evolution* **20**(3), 408–417.

Radinsky LB (1969) The Early Evolution of the Perissodactyla. *Evolution* **23**(2), 308–3281.

Rafferty KL, Herring SW, Marshall CD (1999) Craniofacial sutures: morphology, growth, and *in vivo* masticatory strains. *J Morphol* **242**, 167–179.

Rafferty KL, Herring SW, Marshall CD (2003) Biomechanics of the rostrum and the role of facial sutures. *J Morphol* **257**(1), 33–44.

R Development Core Team (2015) *R: a language and environment for statistial computing*. Vienna, Austria: R. Foundation for Statistical computing.

Simpson GG (1945) Notes on Pleistocene and recent Tapirs. *Bull Am Mus Nat Hist* **86**, 34–81.

Sisson S, Grossman JD (1982) *Anatomía de los animales domésticos. Tomo 1*. 5th edn. Barcelona: Salvat. pp. 1022.

Sun Z, Lee E, Herring SW (2004) Cranial sutures and bones: growth and fusion in relation to masticatory strain. *Anat Rec* **276**, 150–161.

Taber A, Chalukian SC, Altrichter M, et al. (2008) El Destino de los Arquitectos de los Bosques Neotropicales: Evaluación de la Distribución y el Estado de Conservación de los Pecaríes Labiados y los Tapires de Tierras Bajas. New York: Grupo Especialista de la CSE/UICN en Cerdos, Pecaríes e Hipopótamos; Grupo Especialista de la CSE/UICN en Tapires; Wildlife Conservation Society; and Wildlife Trust.

Tarnawski BA, Cassini GH, Flores DA (2014a) Allometry of the postnatal cranial ontogeny and sexual dimorphism in *Otaria byronia* (Otariidae). *Acta Theriol* **59**(1), 81–97.

Tarnawski B, Cassini G, Flores D (2014b) Skull allometry and sexual dimorphism in the ontogeny of the southern elephant seal (*Mirounga leonina*). *Can J Zool* **92**, 19–31.

Tarnawski BA, Flores D, Cassini G, et al. (2015) A comparative analysis on cranial ontogeny of South American fur seals (Otariidae: *Arctocephalus*). *Zool J Linn Soc* 173, 249–269.

Traeholt C, Novarino W, bin Saaban S, et al. (2016). *Tapirus indicus*. The IUCN Red List of Threatened Species 2016: e.T21472A45173636. https://doi.org/10.2305/iucn.uk.2016-1.rlts.t21472a45173636.en (accessed on 14 February 2017).

Voss RS, Helgen KM, Jansa SA (2014) Extraordinary claims require extraordinary evidence: a comment on Cozzuol et al. (2013). *J Mammal* **95**(4), 893–898.

Wall WP (1980) Cranial evidence for a proboscis in *Cadurcodon* and a review of snout structure in the family Amynodontidae (Perissodactyla, Thinocerotoidea). *J Paleo* **54**(5), 968–977.

Wilson DE, Reeder DM (2005) *Mammal species of the world*. 3rd edn. Baltimore: Johns Hopkins University Press.

Witmer LM, Sampson SD, Solounias N (1999) The proboscis of tapirs (Mammalia: Perissodactyla): a case study in novel narial anatomy. *J Zool Soc Lond* **249**, 249–267.